Protein Science (1998), 7:746–757. Cambridge University Press. Printed in the USA.

Structural and functional characterization of recombinant human cellular retinaldehyde-binding protein

JOHN W. CRABB,[1,5] ANNE CARLSON,[2] YANG CHEN,[1] STEVE GOLDFLAM,[1] RICHARD INTRES,[1,6] KAREN A. WEST,[1] JEFFREY D. HULMES,[1] JAMES T. KAPRON,[1,7] LINDA A. LUCK,[1,5] JOSEPH HORWITZ,[3] AND DEAN BOK[2–4]

[1]Adirondack Biomedical Research Institute, Lake Placid, New York 12946
[2]Department of Neurobiology, UCLA, Los Angeles, California
[3]Jules Stein Eye Institute, UCLA, Los Angeles, California
[4]Brain Research Institute, UCLA, Los Angeles, California
[5]Department of Biology, Clarkson University, Potsdam, New York 13699

(RECEIVED September 23, 1997; ACCEPTED November 20, 1997)

Abstract

Cellular retinaldehyde-binding protein (CRALBP) is abundant in the retinal pigment epithelium (RPE) and Müller cells of the retina where it is thought to function in retinoid metabolism and visual pigment regeneration. The protein carries 11-*cis*-retinal and/or 11-*cis*-retinol as endogenous ligands in the RPE and retina and mutations in human CRALBP that destroy retinoid binding functionality have been linked to autosomal recessive retinitis pigmentosa. CRALBP is also present in brain without endogenous retinoids, suggesting other ligands and physiological roles exist for the protein. Human recombinant cellular retinaldehyde-binding protein (rCRALBP) has been over expressed as non-fusion and fusion proteins in *Escherichia coli* from pET3a and pET19b vectors, respectively. The recombinant proteins typically constitute 15–20% of the soluble bacterial lysate protein and after purification, yield about 3–8 mg per liter of bacterial culture. Liquid chromatography electrospray mass spectrometry, amino acid analysis, and Edman degradation were used to demonstrate that rCRALBP exhibits the correct primary structure and mass. Circular dichroism, retinoid HPLC, UV-visible absorption spectroscopy, and solution state ^{19}F-NMR were used to characterize the secondary structure and retinoid binding properties of rCRALBP. Human rCRALBP appears virtually identical to bovine retinal CRALBP in terms of secondary structure, thermal stability, and stereoselective retinoid-binding properties. Ligand-dependent conformational changes appear to influence a newly detected difference in the bathochromic shift exhibited by bovine and human CRALBP when complexed with 9-*cis*-retinal. These recombinant preparations provide valid models for human CRALBP structure–function studies.

Keywords: amino acid analysis; circular dichroism; mass spectrometry; NMR; recombinant; retinoids; secondary structure; visual cycle

CRALBP is thought to serve as a substrate carrier protein in the mammalian visual cycle, modulating whether 11-*cis*-retinol (11-*cis*-Rol) is stored as an ester in the retinal pigment epithelium (RPE) or oxidized by 11-*cis*-Rol dehydrogenase to 11-*cis*-retinal (11-*cis*-Ral) for visual pigment regeneration (Saari et al., 1994). In the RPE and Müller cells of the retina, CRALBP endogenously carries 11-*cis*-retinoids, the isomers of vitamin A utilized for phototransduction. However, CRALBP is not always associated with a retinoid ligand, and more than one physiological role for the protein appears likely (Saari et al., 1997). The protein is also present in ciliary body, cornea, pineal gland, optic nerve, brain, transiently in iris, but not in the rod and cone photoreceptor cells. Notably, retinoids have not been found associated with the brain-derived protein and in developing retina and RPE, CRALBP is expressed before the tissues contain 11-*cis*-retinoids or the isomerase responsible for generating 11-*cis*-retinoids (Saari et al., 1997). CRALBP would appear to serve functions unrelated to visual pigment regeneration in brain and tissues not involved in the visual cycle.

CRALBP was detected first in bovine retina based on its ability to form complexes with exogenous radioactive 11-*cis*-Ral (Futter-

Reprint requests to: John W. Crabb, Protein Chemistry, Adirondack Biomedical Research Institute, 10 Old Barn Road, Lake Placid, New York 12946; e-mail: jcrabb@cell-science.org.

[6]Present address: Berkshire Medical Center, Pittsfield, Massachusetts 01201.

[7]Present address: Advanced Bioanalytical Services, Ithaca, New York 14850.

Abbreviations: CD, circular dichroism; CRALBP, cellular retinaldehyde-binding protein; CRBP, cellular retinol-binding protein; DTT, dithiothreitol; EDTA, ethylene diamine tetraacetate; HTP, hydroxylapatite; IPTG, isopropyl-β-D-thiogalactopyranoside; IRBP, interphotoreceptor retinoid-binding protein; LC ESMS, liquid chromatography electrospray mass spectrometry; MES, 2(N-morphino)ethane sulfonic acid; MOPS, 3(N-morpholino)propane sulfonic acid; Ral, retinaldehyde; RBP, serum retinol binding protein; Rol, retinol; RPE, retinal pigment epithelium; rCRALBP, recombinant cellular retinaldehyde-binding protein; RP-HPLC, reverse-phase high-performance liquid chromatography; rt, retention time; SDS-PAGE, Sodium dodecyl sulfate polyacrylamide gel electrophoresis.

man et al., 1977) and was subsequently purified and shown to carrying endogenous ligands (Stubbs et al., 1979). Bovine CRALBP structure–function studies have identified the endogenous ligands associated with the protein from RPE and neural retina (Saari et al., 1982), defined ligand stereo-selectivity and photo-sensitivity (Saari & Bredberg, 1987), developed a topological and epitope map (Crabb et al., 1991), and established *in vitro* evidence for a substrate carrier function in RPE (Saari & Bredberg, 1982; Saari et al., 1994). The primary structure of bovine CRALBP has been determined directly (Crabb et al., 1988a), the bovine and human cDNAs cloned (Crabb et al., 1988b) and the human genomic DNA characterized (Intres et al., 1994); human and bovine CRALBP are 92% identical in amino acid sequence. Other proteins exhibiting modest sequence identity with CRALBP (25–33% over 209–259 amino acids) include (a) the putative substrate targeting domain of cytoplasmic protein tyrosine phosphatase (Gu et al., 1992); (b) SEC14p, a yeast protein involved in secretion from the Golgi complex (Salama et al., 1990); and (c) α-tocopherol transfer protein, a protein that appears to transfer α-tocopherol between membranes in rat liver (Sato et al., 1993). Squid retinal-binding protein, a protein thought to be involved in retinoid transport and photoproduct regeneration in squid retina (Ozaki et al., 1994), also shares limited homology with CRALBP (about 26% identity over 106 residues). No significant sequence identity exists with other retinoid-binding proteins or the visual pigments.

As part of ongoing efforts to better understand the normal function of CRALBP, we have developed a recombinant source of human CRALBP to enhance the availability of the human protein for structure–function studies. These recombinant preparations are beginning to prove useful in both basic and clinically relevant studies. Notably, a recent genetic linkage study showed that an Arg to Gln mutation at residue 150 in human CRALBP can cause autosomal recessive retinitis pigmentosa and preparation of mutant R150Q rCRALBP demonstrated a lack of retinoid-binding function (Maw et al., 1997). Other preliminary studies with the recombinant protein have localized the retinoid-binding domain to the C-terminal region (Chen et al., 1994), characterized ligand interactions by NMR (Luck et al., 1997), and identified residues within the retinoid-binding pocket (Crabb et al., 1996, 1997a). This report describes the original expression cloning of human rCRALBP, documents the structural and functional resemblance of the recombinant and bovine gene products, and addresses the molecular basis of the bathochromic shift exhibited by the CRALBP retinoid ligand.

Results

Expression or rCRALBP

Wild-type rCRALBP was expressed as fusion and non-fusion proteins in *Escherichia coli* strain BL21(DE3)LysS using pET19b and pET3a vectors, respectively. Non-fusion human rCRALBP was expressed as a predicted 316 amino acid protein (Crabb et al., 1988b), and fusion human rCRALBP as a predicted 339 amino acid protein with an N-terminal histidine tag sequence. The 23 residue N-terminal extension facilitates protein purification by nickel affinity chromatography; all but two residues can be removed by proteolysis with enterokinase (Novagen, Inc., Madison, WI). The over-expression of rCRALBP in the soluble bacterial cell lysate fractions of pET3a (Supplementary Fig. 1) and pET19b (Supplementary Fig. 2) cultures was demonstrated by SDS-PAGE and Western blot analysis; very little "leaky" expression was apparent in the absence of induction with isopropyl-β-D-thiogalactopyranoside (IPTG). Densitometric analysis of SDS-PAGE Coomassie Blue staining intensity from multiple preparations indicated that the expression level of rCRALBP varied from 10–50% of total cellular protein, depending on culture conditions and specific clone analyzed (data not shown). Typically, rCRALBP accounted for 15–20% of the total soluble lysate protein obtained in 1.2 L cultures grown 3 h after induction in LB media at 37 °C in shaking 2.8 L Fernbach flasks (Crabb et al., 1998b). Under these conditions 50% of the expressed wild-type rCRALBP typically remained in the soluble fraction based on SDS-PAGE Coomassie Blue staining.

Purification and N-terminal sequence

Methods for purifying rCRALBP have been described elsewhere (Crabb et al., 1998b). Non-fusion rCRALBP was purified from the soluble bacterial lysate fraction following labeling with 11-*cis*-Ral using DEAE-cellulose, hydroxylapatite, and Mono Q chromatography (Supplementary Fig. 3). Final preparations of the non-fusion rCRALBP sometimes showed a doublet in SDS-PAGE (Supplementary Fig. 3D) and when analyzed by Edman degradation yielded the N-terminal sequence of human CRALBP (SEGVGTFRM...) with a minor truncated component starting at residue 8 (RMVPEEEQEL). The truncation had no apparent effect on retinoid binding properties and may be due to the lability of the N-terminal region of CRALBP to proteolysis (Crabb et al., 1991). Non-fusion rCRALBP was expressed without the N-terminal acetyl modification present in bovine retinal CRALBP (Crabb et al., 1988a). The fusion rCRALBP was purified from *E. coli* lysates by a combination of DEAE-cellulose and nickel affinity chromatography (Supplementary Fig. 4). The majority of rCRALBP typically eluted from the Ni-NTA column in early fractions (i.e., in the first 2–5 mL), with trailing amounts eluting after 20 mL of elution buffer (Supplementary Fig. 4). Very late eluting fractions have been found to contain apo rCRALBP without bound retinoid, suggesting that these fractions contain misfolded rCRALBP. Edman sequence analysis of the purified fusion rCRALBP demonstrated an N-terminal sequence identical to the His-tag sequence (GHHHHHHHHH...). These methods typically yield about 7–8 mg of purified non-fusion rCRALBP per liter of bacterial culture and about 3–4 mg of purified fusion rCRALBP per liter of culture. The lower yield of the fusion protein may be associated with very tight binding with the nickel affinity support.

Molecular weight, amino acid composition, and primary structure

Analysis of the purified rCRALBPs by liquid chromatography electrospray mass spectrometry (LC ESMS) and amino acid analysis indicated that complete polypeptides with the predicted amino acids had been produced. Intact non-fusion and fusion rCRALBP were found by LC ESMS to exhibit molecular weights of 36,347 ± 4 and 39,114 ± 4, respectively, in excellent agreement with the masses of the apo proteins calculated from their amino acid sequences, namely, 36,343 and 39,110, respectively (Crabb et al., 1997b). Amino acid analysis of the purified proteins yielded compositional data in excellent agreement with the predicted compositions (Table 1). The complete primary structure of the purified fusion rCRALBP was verified by LC ESMS (Fig. 1, and Supplementary Mass Spectra); tryptic peptides encompassing the protein

Table 1. *Amino acid compositions of human rCRALBP*

Amino acid		Residues per molecule			
		Fusion rCRALBP[a] M_r = 39,110		Nonfusion rCRALBP[b] M_r = 36,343	
		Known	Experimental[c]	Known	Experimental[c]
Asx	(D+N)	29	28.2	25	22.8
Glx	(E+Q)	57	60.4	57	53.4
Ser	(S)	17	16.6	15	14.3
Gly	(G)	21	27.2	19	23.0
His	(H)	17	14.6	5	5.3
Arg	(R)	20	22.6	20	21.8
Thr	(T)	15	15.2	15	14.9
Ala	(A)	23	25.5	23	25.4
Pro	(P)	13	12.5	13	13.3
Tyr	(Y)	10	8.8	10	8.8
Val	(V)	20	19.1	20	18.8
Met	(M)	7	7.5	6	6.3
Ile	(I)	14	11.3	13	10.2
Leu	(L)	30	33.2	30	31.8
Phe	(F)	24	24.1	24	22.9
Lys	(K)	16	16.5	15	15.5
Total[d]		333	345	310	308
Amount hydrolyzed/analyzed (μg)		1.5			1.9
Average compositional error (%)[e]		9.1			6.9

[a]Fusion rCRALBP was purified by DEAE and Ni affinity chromatographies.
[b]Non-fusion rCRALBP was purified by DEAE, HTP, and MonQ chromatographies.
[c]Experimental compositions were determined by phenylthiocarbamyl-amino acid analysis as described in Materials and methods; the known compositions are from sequence data.
[d]Cys and Trp were not included.
[e]Calculated as defined in Crabb et al. (1997b).

were identified with an average deviation of less than 0.3 Da between calculated and observed peptide masses (Table 2). No evidence was found for chemical or post-translational modifications other than from carboxyamidomethylation introduced by experimental design for the structural analysis.

Secondary structure and thermal stability studies

Far UV CD analysis of purified native bovine and fusion recombinant CRALBP demonstrated essentially identical spectra (Fig. 2A), with no significant differences apparent in secondary structure composition. The following estimates of secondary structure were calculated using the LINCOMB algorithm for native bovine and human rCRALBP, respectively: % α helix (bovine, 32 ± 2; human, 34 ± 1); % β sheet (bovine, 14 ± 2; human, 12 ± 4), % β turn (bovine, 29 ± 5; human; 24 ± 6), % unordered (bovine, 25 ± 3; human, 31 ± 3), and % random (bovine, 54 ± 2; human, 55 ± 3). Here the sum of the β turn and unordered structure is equivalent to random structure; three samples of each holoprotein were analyzed with bound 11-*cis*-Ral, 11-*cis*-Rol or both. The far UV CD spectra also exhibit no significant difference for rCRALBP complexed either 11-*cis*-Rol, 11-*cis*-Ral, a mixture of the two retinoids or as the apo protein (Fig. 2B). The lack of a major difference in secondary structure between apo and holo forms of rCRALBP is consistent with heteronuclear single quantum correlation NMR spectra of ^{15}N-rCRALBP with and without 11-*cis*-Ral (Luck et al., 1997). The NMR analysis showed that the protein undergoes a specific, localized change upon removal of the ligand, and that the global rCRALBP conformation is relatively unaffected by ligand.

Increasing temperatures affected the shape and intensity of the far UV CD spectra of CRALBP (Fig. 3A). The highest temperature found not to induce a change in the far UV CD spectra for the apo proteins was 39 °C (for both bovine and recombinant human CRALBP). For both holo proteins, a temperature of 50 ± 2 °C was required for a detectable change, indicating that the holo protein structures are more stable than the apo proteins. To evaluate whether temperature induced changes in the far UV CD spectra had any impact on retinoid binding function, apo human rCRALBP was incubated at 4, 40, and 53 °C for 5 min, then 11-*cis*-Ral was added to each, the mixtures incubated at 4 °C for 10 min, and near-UV-visible CD spectra recorded. The CD spectra from the sample maintained at 4 °C exhibited the characteristic 425 nm peak maximum and 320 nm *cis* band of 11-*cis*-Ral bound to CRALBP; the spectra from the 40 °C sample was also similar but reduced in intensity (Fig. 3B). The sample incubated at 53 °C failed to bind 11-*cis*-Ral, as evidenced by a spectra similar to apo CRALBP.

Retinoid binding properties

In the dark, purified wild-type fusion and non-fusion human rCRALBP and bovine retinal CRALBP bind 11-*cis*-Ral in the same, specific manner, evidenced by the bathochromic shift in the absorbance of the retinoid from 380 nm (the approximate absorbance maxima for free 11-*cis*-Ral in aqueous solution) to 425 nm (Fig. 4). The 425-nm peak maximum is characteristic of bovine CRALBP bound 11-*cis*-Ral (Stubbs et al., 1979). Upon exposure to bleaching illumination, the absorbance of the CRALBP·11-*cis*-Ral complex shifts from 425 to 380 nm due to the production of free all-*trans*-Ral. The absorption spectra of human fusion rCRALBP complexed with 9-*cis*-Ral is shown in Figure 4D, and contains a chromophoric absorbance maximum at 400 nm, slightly less than the 405 nm chromophoric absorbance maximum exhibited by bovine retinal CRALBP (Saari & Bredberg, 1987). Upon bleaching, rCRALBP bound 9-*cis*-Ral is isomerized to free all-*trans*-Ral with a 380 nm absorbance maximum (Fig. 4D). Near-UV circular dichroism was also used to compare the retinoid binding properties of bovine retinal and human recombinant CRALBP; characteristic maxima for the proteins complexed with 11-*cis*-Ral or 11-*cis*-Rol (425 and 340 nm, respectively) can be seen in Figure 5 along with less predominant *cis* bands from 11-*cis*-Ral (320 nm) and 11-*cis*-Rol (290 nm). When CRALBP is complexed with a mixture of 11-*cis*-Rol and 11-*cis*-Ral, both maxima are exhibited (Fig. 5). The absorption, bleaching, and near-UV spectra in Figures 4 and 5 are virtually identical for human rCRALBP and bovine retinal CRALBP.

The stereoselectivity or retinoid isomer binding preference of rCRALBP was also evaluated by near-UV-visible CD after presenting a variety of retinoids to apo CRALBP (Fig. 5). There are two significant advantages in this experimental design relative to previous CRALBP retinoid binding studies. First, retinoids in solution do not exhibit a CD signal in the near-UV-visible spectral range by themselves, nor does apo CRALBP; consequently, only retinoid–protein complexes are detected, and are unobscured by excess, unbound retinoid in the solution. Second, while bovine apo

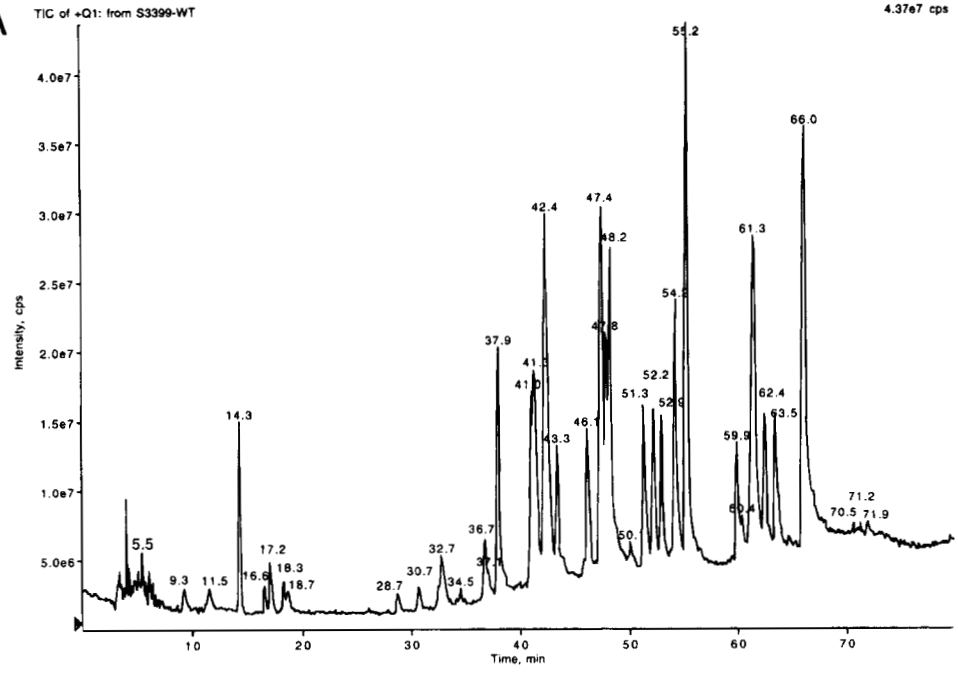

Fig. 1. LC ESMS analysis of rCRALBP. Wild-type fusion human rCRALBP was carboxyamidomethylated, digested with trypsin and ~6 μg of the digest analyzed by LC ESMS with a PE Sciex API 300 triple quadrupole electrospray mass spectrometer. **A:** The total ion current (TIC) for the full scan m/z 250–2,200 is shown. Supplementary mass spectra for all peaks labeled by retention time are available in the Electronic Appendix. Peptides identified by mass that encompass rCRALBP are listed in Table 2 by sequence position and retention time. Other rCRALBP partial proteolysis fragments and peptides eluting at more than one position can be found in the Supplementary Mass Spectra. **B:** Tryptic peptides were also identified using the computer program PeptideMap (version 2.2, PE Sciex). Slash marks (/) indicate tryptic cleavage sites; wavy lines indicate identified peptides.

CRALBP is difficult to prepare from the holoprotein due to instability, human apo fusion rCRALBP can be readily obtained from bacterial lysates in the absence of exogenous retinoid via affinity chromatography. The results of the CD analysis of retinoid binding analysis are presented in Figure 5 and show that only 11-*cis*-Ral and 11-*cis*-Rol were found to form specific complexes with recombinant human or bovine retinal CRALBP. Other retinoids that were tested and which rCRALBP failed to bind include 9-*cis*-Rol, 13-*cis*-Ral, 13-*cis*-Rol, all-*trans*-Ral, and all-*trans*-Rol (data not shown). These retinoid binding properties are in excellent agreement with those previously described for bovine retinal CRALBP (Saari & Bredberg, 1987).

To further characterize rCRALBP ligand binding properties and to confirm the identity of the ligand, the purified holo protein was extracted with hexane and the extract analyzed by isocratic RP HPLC. Although only 11-*cis*-Ral was added to the bacterial cell lysate prior to purification, the components of the hexane extract co-eluted in the HPLC analysis with both 11-*cis*-Ral and 11-*cis*-

Table 2. *Peptides identified by LS ESMS from human rCRALBP*[a]

Residues	Retention time (min)	Calculated mass	Observed mass	Error (Da)	Sequence
1–31	42.4	3,618.8av	3,619.0	0.2	GHHHHHHHHHHSSGHIDDDDKHMSEGVGTFR⟩M
22–31	50.1	1,119.5	1,119.8	0.3	K⟨HMSEGVGTFR⟩M
32–41	41.3	1,258.6	1,258.8	0.2	R⟨MVPEEEQELR⟩A
42–50	41.0	1,030.6	1,030.8	0.2	R⟨AQLEQLTTK⟩D
51–64	47.4	1,565.7	1,566.0	0.3	K⟨DHGPVFGPCSQLPR⟩H
65–69	17.2	625.4	625.5	0.1	R⟨HTLQK⟩A
70–77	30.7	973.5	973.6	0.1	K⟨AKDELNER⟩E
70–86	37.9	2,074.2av	2,074.3	0.1	K⟨AKDELNER/EETREEAVR⟩E
78–86	28.7	1,117.5	1,117.6	0.1	R⟨EETREEAVR⟩E
82–86	17.2	602.3	602.3	0	R⟨EEAVR⟩E
87–109	59.9	2,429.7av	2,429.9	0.2	R⟨ELQEMVQAQAASGEELAVAVAER⟩V
110–113	9.3	502.3	502.3	0	R⟨VQEK⟩D
110–120	50.1	1,324.7	1,325.0	0.3	R⟨VQEKDSGFFLR⟩A
114–120	51.3	840.4	840.5	0.1	K⟨DSGFFLR⟩F
121–123	32.7	434.3	434.4	0.1	R⟨FIR⟩A
124–126	5.5	373.2	373.2	0	R⟨ARK⟩F
126–131	36.7	719.4	719.5	0.1	R⟨KFNVGR⟩A
127–131	37.0	591.3	591.4	0.1	K⟨FNVGR⟩A
132–137	46.1	763.4	763.5	0.1	R⟨AYELLR⟩G
138–143	43.3	754.4	754.5	0.1	R⟨GYVNFR⟩L
144–159	61.3	1,862.9	1,863.0	0.1	R⟨LQYPELFDSLSPEAVR⟩C
160–173	48.2	1,508.7	1,509.0	0.3	R⟨CTIEAGYPGVLSSR⟩D
174–178	16.6	637.3	637.5	0.2	R⟨DKYGR⟩V
176–178	16.6	394.2	394.3	0.1	K⟨YGR⟩V
179–208	71.9	3,722.3av	3,722.6	0.3	R⟨VVMLFNIENWQSQEITFDEILQAYCFILEK⟩L
209–227	62.4	2,311.6av	2,311.8	0.2	K⟨LLENEETQINGFCIIENFK⟩G
228–238	47.8	1,208.6	1,208.8	0.2	K⟨GFTMQQAASLR⟩T
239–243	18.7	590.3	590.4	0.1	R⟨TSDLR⟩K
239–244	18.3	718.4	718.5	0.1	R⟨TSDLRK⟩M
244–256	52.9	1,536.7	1,537.0	0.3	R⟨KMVDMLQDSFPAR⟩F
245–256	54.2	1,408.6	1,408.8	0.2	K⟨MVDMLQDSFPAR⟩F
257–258	14.3	293.2	293.2	0	R⟨FK⟩A
259–281	66.0	2,851.3av	2,851.6	0.3	K⟨AIHFIHQPWYFTTTYNVVKPFLK⟩S
282–287	34.5	744.5	744.7	0.2	K⟨SKLLER⟩V
288–317	66.0	3,310.6av	3,310.6	0	R⟨VFVHGDDLSGFYQEIDENILPSDFGGTLPK⟩Y
318–321	11.5	481.2	481.3	0.1	K⟨YDGK⟩A
322–339	55.2	1,890.9	1,891.1	0.2	K⟨AVAEQLFGPQAQAENTAF (C-terminus)

[a]Fusion rCRALBP peptides identified by LC ESMS in Figure 1A are listed by residues, total ion current retention time, calculated and observed masses, and amino acid sequences. Calculated masses are monoisotopic unless indicated as chemical average masses (av). Error refers to the difference between the observed and calculated masses The symbols (⟨,⟩) denote the proteolytic cleavage sites. Residues 1–23 constitute the N-terminal His tag extension. Mass spectra for all listed peptides are available in the Electronic Appendix.

Rol and exhibited UV-visible absorption spectra identical with the authentic free 11-*cis* retinoids (Fig. 6). This observation indicates that partial reduction of 11-*cis*-Ral occurred during the preparation of rCRALBP either before and/or after the retinoid was protein bound.

rCRALBP conformational changes associated with interactions with 11-*cis*-Ral were monitored by solution state ^{19}F-Trp NMR before and after exposure to bleaching illumination (Fig. 7). Before each NMR analysis, the presence or absence of ligand in the rCRALBP retinoid binding pocket was verified by UV-visible spectral analysis (as in Fig. 4). rCRALBP contains two Trp residues. The two ^{19}F chemical shift changes of the 5-fluorotryptophan–labeled residues apparent in the spectra before and after bleaching (Fig. 7) are significant, and suggest that the Trp residues undergo ligand-dependent conformational change.

Discussion

A bacterial recombinant protein production system has been established to provide a source of human CRALBP for structure function studies. Expression levels of the proteins are dependent upon specific clones and culture conditions (Supplementary Figs. 1 and 2) but milligram amounts of the purified rCRALBPs are typically recovered. Richer growth media and more vigorous culture conditions have yielded greater bacterial cell mass but with increased localization of wild-type rCRALBP in the insoluble inclusion body fraction (Crabb et al., 1998). Reduced solubility of mutant rCRALBP relative to the wild-type protein has also been observed (Maw et al., 1997). The solubility of some mutant rCRALBPs has been enhanced by growing the bacterial cultures at room temperature in a minimal medium (i.e., 10 g/L bacto-

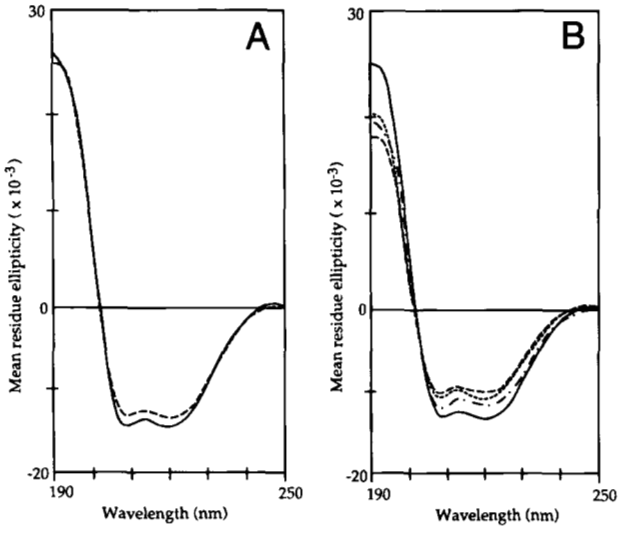

Fig. 2. Far-UV CD spectra of purified bovine retinal and human rCRALBP. **A:** Bovine retinal (—) and human rCRALBP (– – –) complexed with 11-*cis*-Ral. Protein concentrations were 5.5–5.7 μM based on the 280 nm absorbance and amino acid analysis. **B:** Human rCRALBP complexed with 11-*cis*-Ral (—), 11-*cis*-Rol (– – –), a mixture of 11-*cis*-Ral and 11-*cis*-Rol (- - -), or in the apo form (- · -- -- · -). Protein concentrations were all within 4.0–5.7 μM.

tryptone, 1 g/L bacto-yeast extract, and 2 g/L sodium chloride) (Crabb et al., 1998).

The quality of the human rCRALBP preparations and similarity with bovine retinal CRALBP was established by rigorous structural characterization. The sensitivity of the retinoid ligands to photo-isomerization complicated the protein chemical analyses and required that purification of the holo proteins (Supplementary Figs. 3 and 4) and many subsequent measurements be made in the dark, under dim red illumination. The intact fusion and non-fusion rCRALBPs were shown to exhibit the cDNA-predicted molecular weights (Crabb et al., 1998) and compositions (Table 1). The complete primary structure of the fusion protein was verified and shown not to contain unexpected chemical or posttranslational modifications (Fig. 1, Table 2, and Supplementary Mass Spectra). No significant difference in secondary structure was detected by far-UV CD analysis (Fig. 2) of bovine retinal and human rCRALBP. Comparison of the predicted secondary structure of CRALBP with published values for CRBP (Cowan et al., 1993), RBP (Cowan et al., 1990), and IRBP (Adler et al., 1985) suggest that CRALBP may be unique in having the highest α-helical content among these retinoid-binding proteins. Thermal stability studies (Fig. 3) revealed no significant differences between bovine retinal and human recombinant holo CRALBP, and confirmed the apo protein to be less stable than holo CRALBP.

The functional quality of the human recombinant CRALBP preparations was also established. UV-visible absorption measurements show that the fusion and non-fusion forms of rCRALBP bind the same limited complement of retinoids as the bovine retinal CRALBP, namely 11-*cis*-Ral, 11-*cis*-Rol, and 9-*cis*-Ral (Figs. 4–6). Upon exposure to bleaching illumination, holo CRALBPs complexed with either 11-*cis*-Ral or 9-*cis*-Ral were shown to generate free all-*trans*-retinaldehyde, as does bovine CRALBP (Saari & Bredberg, 1987). The spectral ratio for fully saturated holoprotein can be approximated by the ratio of relevant extinction coefficients; for 11-*cis*-Ral–labeled rCRALBP $\epsilon^{280}/\epsilon^{425} = 3.2$ and for 9-*cis*-Ral–labeled rCRALBP $\epsilon^{280}/\epsilon^{400} = 2.2$. Observed A_{280}/A_{425} and A_{280}/A_{400} spectral ratios vary with rCRALBP preparation and sample handling but with high purity protein and ligand, can approximate 1:1 binding stoichiometry for both 11-*cis*-Ral and 9-*cis*-Ral (Fig. 4). Retinoid binding properties were also evaluated by near-UV CD spectroscopy. This measurement was specific for the retinoid·protein complex, and showed that rCRALBP complexed

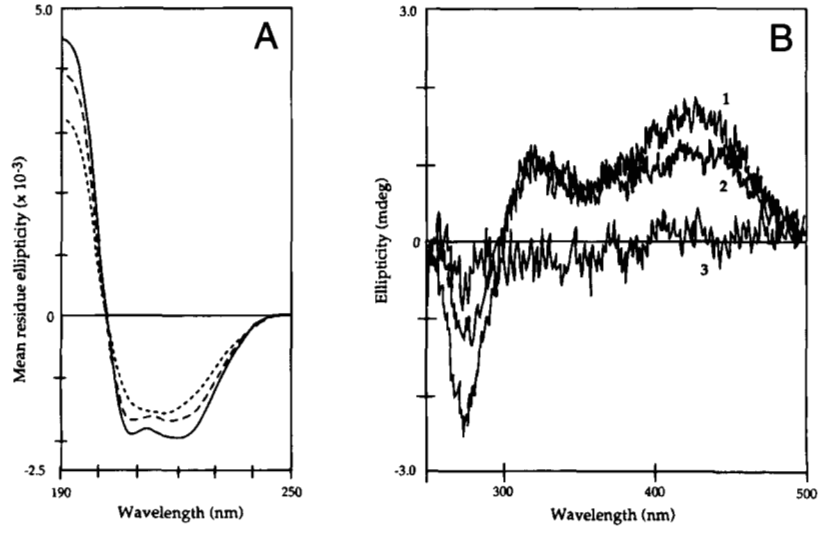

Fig. 3. Change in human rCRALBP CD spectra with increasing temperature. **A:** Far-UV CD spectra of apo rCRALBP at 25 °C (—), 39 °C (– – –), and 52 °C (- - -). **B:** Near-UV-visible CD spectra of apo rCRALBP incubated for 5 min at 4 °C (1), 40 °C (2), or 53 °C (3) followed by a 10-min incubation with 11-*cis*-Ral at 4 °C. Protein concentrations were ~2.8 μM prior to heat treatment. (Compare the spectra in panel B to those in Fig. 5A.)

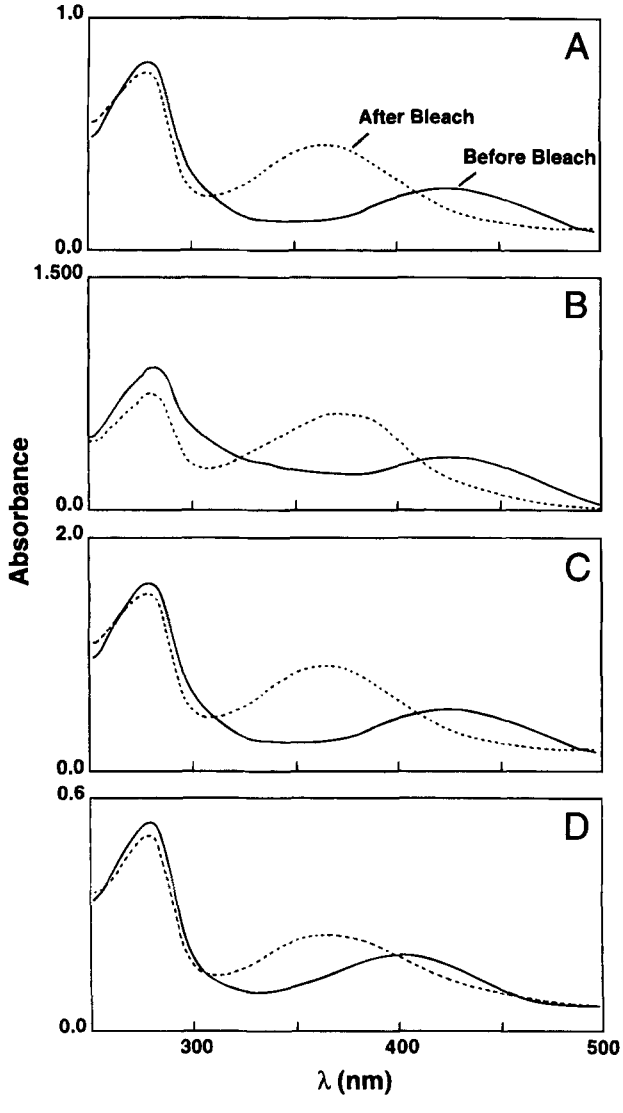

Fig. 4. UV-visible absorption spectra. UV-visible absorption spectra are shown before and after exposure to bleaching illumination of purified (**A**) non-fusion rCRALBP (18.4 μM, A_{280}/A_{425} = 3.1); (**B**) fusion rCRALBP (32.5 μM, A_{280}/A_{425} = 2.8), and (**C**) bovine retinal CRALBP (38 μM, A_{280}/A_{425} = 3.1). The proteins were complexed with 11-*cis*-Ral in these three spectra and exhibit the characteristic chromophoric maxima at 425 nm for CRALBP bound 11-*cis*-Ral. Upon bleaching, the absorbance maxima shift to 380 nm due to photoisomerization of the retinoid and production of unbound all-*trans*-Ral. Panel D shows the absorption spectra of fusion rCRALBP complexed with 9-*cis*-Ral (11.9 μM, A_{280}/A_{400} = 2.7). The chromophoric maximum for human rCRALBP-bound 9-*cis*-Ral is 400 nm; this maximum shifts to 380 upon bleaching due to the production of free all-*trans*-Ral.

with 11-*cis*-retinoids produced the same maxima as bovine retinal CRALBP.

An intriguing difference between bovine and human CRALBP concerns the chromophoric maxima when complexed with 9-*cis*-Ral. Bovine CRALBP exhibits a slightly red shifted maximum of 405 nm with 9-*cis*-Ral (Saari & Bredberg, 1987) relative to the 400 nm maximum of human rCRALBP (Fig. 4D). The 8% difference in the bovine and human CRALBP sequences would appear to be a basis for the different red shifts, but no difference exists in the chromophoric maxima of bovine and human CRALBP complexed with 11-*cis*-Ral (i.e., 425 nm). Why does one ligand exhibit a species specific absorption difference and the other does not? Notably, Saari and Bredberg (1987) have ranked the relative retinoid binding affinity of bovine CRALBP: 11-*cis*-Ral > 11-*cis*-Rol > 9-*cis*-Ral. While CRALBP binds 9-*cis*-Ral, it does not bind 9-*cis*-Rol. Based on relative retinoid binding affinity, we predict a looser binding pocket structure for CRALBP complexed with 9-*cis*-Ral than with 11-*cis*-Ral, and this may effect the chromophoric absorption properties. The conformational differences observed by ^{19}F-NMR for rCRALBP with and without 11-*cis*-Ral (Fig. 7) suggest a more open, flexible structure when in the unliganded form. One Trp residue (at −47.2 ppm in Fig. 7) exhibits apparent conformational heterogeneity upon bleaching, and inter-conversion from one form to another is slow relative to the differences in the NMR frequencies. Slow protein motility from one form to another prolongs the availability of various conformations for ligand interactions (Wagner & Wuthrick, 1986). We have also observed ligand-dependent rCRALBP conformational changes by ^{13}C and ^{15}N NMR (Luck et al., 1997). Different three-dimensional structures appear likely for the binding pocket containing 11-*cis*-Ral versus 9-*cis*-Ral. A more relaxed binding pocket structure with 9-*cis*-Ral plus key amino acid substitutions may account for the 5-nm difference in chromophoric maxima between bovine and human CRALBP. A more constrained binding pocket structure with 11-*cis*-Ral, which sequesters the ligand further away from residue interchanges, may account for the identical red shifts observed between bovine and human CRALBP.

Which amino acid residues contribute to the molecular basis of the CRALBP bathochromic shift in ligand absorbance? Recent studies have demonstrated that hydroxyl-bearing amino acids increase the red shift of 11-*cis*-Ral bound to human red and green cone pigments (Asenjo et al., 1994). Overall, bovine CRALBP contains 41 hydroxyl-bearing amino acids, one more than human CRALBP (Crabb et al., 1988b); interchanges that increase the hydroxyl amino acid content of the bovine protein occur at residue positions 241 (bovine Tyr, human His), 274 (bovine Ser, human Gly), and 311 (bovine Thr, human Ala). Based on the apparent ligand dependent conformational change at nearby Trp 244 in human rCRALBP (Fig. 7), Tyr 241 may be responsible in part for the deeper red shift exhibited by the bovine versus the human protein complexed with 9-*cis*-Ral. Site-directed mutagenesis and retinoid binding studies with human rCRALBP will resolve this structure function issue.

CRALBP purifies from bovine retina with endogenous 11-*cis*-Ral and 11-*cis*-Rol in about a 3:1 ratio, respectively (Saari et al., 1982). Holo rCRALBP can be prepared by experimental design to contain both retinoids, as in Figures 2 and 5, but also can be unexpectedly recovered containing both ligands. HPLC and spectral analysis of the ligand extracted from purified rCRALBP (Fig. 6) showed that while exogenously labeled with only 11-*cis*-Ral in the bacterial lysate, rCRALBP was recovered containing about 0.7 mol 11-*cis*-Ral plus about 0.1 mol 11-*cis*-Rol per mole of protein. This is probably due to partial reduction of 11-*cis*-Ral to 11-*cis*-Rol through the action of various dehydrogenases in the bacterial lysate. However, the stereoselectivity of bovine CRALBP has been carefully evaluated; the protein preferentially selects 11-*cis*-Ral from mixtures of retinoids, even when 11-*cis*-Ral is present as a minor component (Saari & Bredberg, 1987). Because the ligand in CRALBP is inaccessible to small chemical reducing agents (Saari & Bredberg, 1982), if reduction of 11-*cis*-Ral oc-

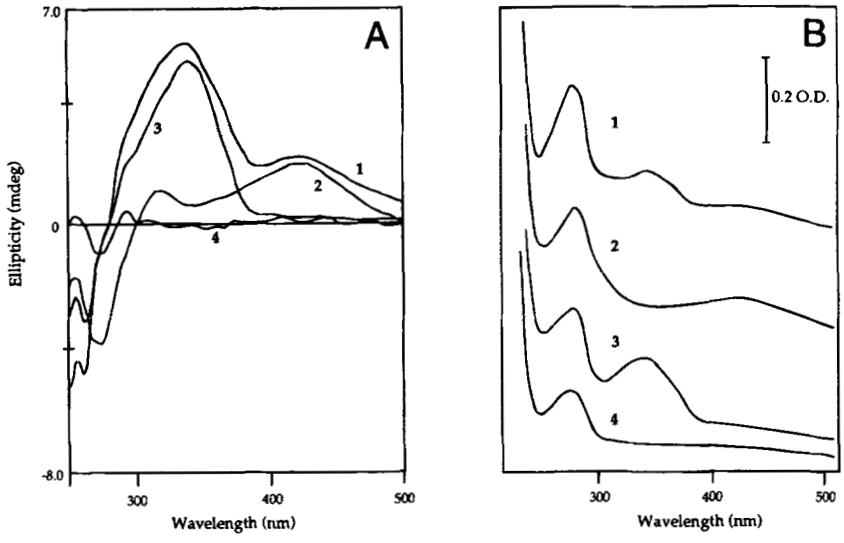

Fig. 5. Near-UV-visible CD spectra (**A**) and absorption spectra (**B**) of rCRALBP. Spectra were recorded with human rCRALBP complexed with a mixture of 11-*cis*-Ral and 11-*cis*-Rol (1), 11-*cis*-Ral (2), 11-*cis*-Rol (3), or as the apo protein (4). Protein concentrations were 4.6–5.8 μM.

curred after the retinoid was bound to rCRALBP in the bacterial lysate, it occurred by an enzymatic process. The recovery of rCRALBP with a single ligand can be maximized by limiting the time involved in retinoid labeling and protein purification time and by using high purity *cis*-retinoids for labeling. Alternatively, the apo rCRALBP may be labeled with ligand following protein purification.

CRALBP is thought to play a vital role in visual pigment regeneration; however, the protein does not always carry a retinoid ligand and is present in tissues not directly involved in the visual cycle (e.g., brain, cornea, ciliary body, and iris). Accordingly, CRALBP may bind hydrophobic ligands other than retinoids and serve multiple functions, some unrelated to vision. The fact that mutations in the human CRALBP gene can cause a loss of retinoid binding capability and result in an inherited ocular disease (i.e., autosomal recessive retinitis pigmentosa) suggests that other pathologies may be associated with nonfunctional CRALBP (e.g, neurodegenerative disorders in the brain). As we learn more about

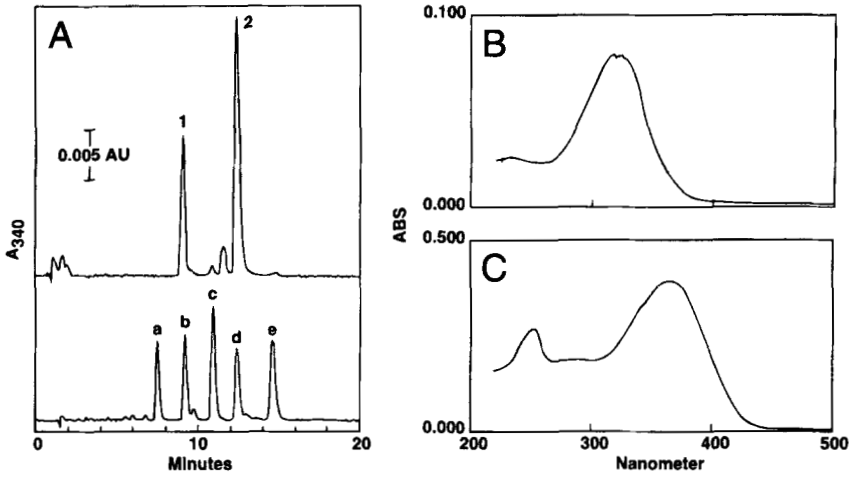

Fig. 6. Retinoid RP HPLC and spectral analysis. **A:** Purified rCRALBP (23.9 nmol) was extracted with 2 vol of hexane and the extract analyzed by isocratic RP HPLC (top profile) as described in Materials and methods. HPLC peak fractions 1 and 2 were collected, extracted with 1 vol of hexane and absorption spectra measured. The lower RP HPLC profile (**A**) is from retinoid standards analyzed under the same chromatography conditions: a, all-*trans*-retinoic acid; b, 11-*cis*-Rol; c, all-*trans*-Rol; d, 11-*cis*-Ral; and e, all-*trans*-Ral. **B:** The absorption spectra of HPLC peak 1 in hexane (λ_{max} = 318 nm) is shown and is identical to that of 11-*cis*-Rol in hexane (Hubbard, 1956). Approximately 2.7 nmol 11-*cis*-Rol was recovered based on 318 nm absorbance and ϵ^{318} = 120 (mg/mL)$^{-1}$ cm^{-1} in hexane (Brown & Wald, 1956). **C:** The absorption spectra of HPLC peak 2 in hexane (λ_{max} = 365 nm, *cis* band at 250 nm) is shown and is identical to 11-*cis*-Ral in hexane (Hubbard, 1956). Approximately 17.6 nmol 11-*cis*-Ral was recovered based on 365 nm absorbance and ϵ^{365nm} = 92.8 (mg/mL)$^{-1}$ cm^{-1} (Oroshnik, 1956).

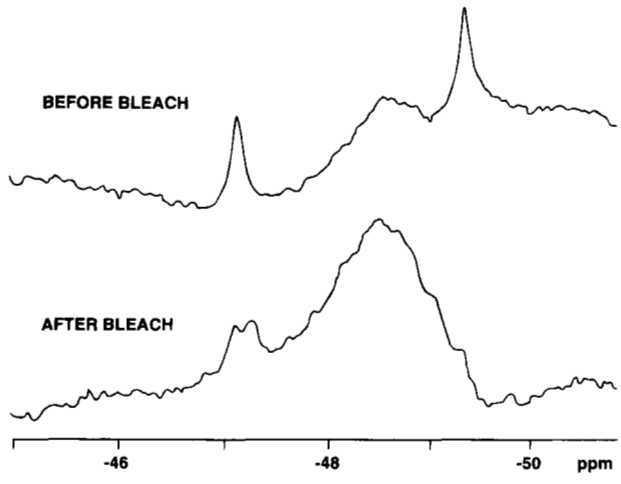

Fig. 7. NMR spectra of ^{19}F-Trp–labeled rCRALBP with and without ligand. Solution-state NMR spectra of CRALBP labeled with ^{19}F-Trp (18 mg/mL) containing bound 11-*cis*-Ral were recorded in the dark. The sample was then exposed to bleaching illumination and re-analyzed without bound ligand. NMR conditions include: pw = 5.9 μs, sw = 5,500 H_z, pre-acquisition delay = 0.5 s; each set of spectra collected 10,000 transients. The two ^{19}F-Trp frequencies visible before bleaching at about −47.2 and −49.5 ppm shift after bleaching. The broad signal between −48 and −49 ppm is indicative of partial denaturation.

the processes in which CRALBP may be involved, these recombinant preparations will be useful in testing hypotheses concerning protein–protein interactions, identifying critical amino acid residues necessary for normal physiological function, and in determining the three-dimensional structure of the protein.

Materials and methods

Materials

Native bovine CRALBP was purified from frozen bovine dark-adapted retinas (J Lawson, Lincoln, NB) according to Saari and Bredberg (1988). 11-*cis*-Ral was obtained from the National Eye Institute, NIH and R Crouch or as a gift from Hoffman-LaRoche (Nutley, New Jersey). Other retinoids (9-*cis*-Ral, 13-*cis*-Ral, and all-*trans*-Ral) were purchased from Sigma Chemical Co. (St. Louis, Missouri). The retinoid alcohol isomers were produced by reducing the corresponding retinoid aldehyde with sodium borohydride.

Expression of rCRALBP

Unique Nde I sites were engineered by PCR at the 5′ and 3′ ends of the 948 bp coding region of the human CRALBP cDNA (Crabb et al., 1988b), polymerase chain reaction (PCR) products subcloned into the pCR 1000 plasmid (Invitrogen, Carlsbad, CA) and transformed/amplified in *E. coli* strain XL1-Blue (Stratagene, La Jolla, CA). Plasmids were isolated (Qiagen, Inc., Valencia, CA), cleaved with Nde I, and the coding region cDNA isolated by preparative electrophoresis, excision and electroelution using an Elutrap (Schleicher and Scheull). The CRALBP cDNA was ligated into Nde I sites in pET3a or pET19b vectors carry the phage T7 RNA polymerase promoter (Studier et al., 1990). The pET3a vector was obtained as a generous gift from F.W. Studier, Brookhaven, and was used to express non-fusion rCRALBP; the pET19b vector was purchased from Novagen, Inc., and was used to express fusion rCRALBP with an N-terminal histidine tag sequence. The orientation of the CRALBP inserts in the pET vectors was determined by PCR analysis of plasmids grown in *E. coli* strain XL1-Blue (Sandhu et al., 1989); vectors carrying the sense orientation insert were transformed into *E. coli* strain BL21(DE3)LysS for recombinant protein expression. Bacterial cells were grown in LB media and production of rCRALBP induced at mid-log phase with 0.5 mM IPTG. Bacterial cells were harvested by centrifugation, washed two to three times with phosphate-buffered saline, and stored as wet cell pellets at −70 °C. Under these conditions, a yield of about 3 g of wet packed cells was obtained per liter of culture. Step-by-step instructions for the production of rCRALBP in bacteria have been described elsewhere (Crabb et al., 1998).

Bacterial lysate protein quantification

Washed, packed cells were suspended in lysis buffer (~3 mL buffer per gram wet cells), incubated with DNase (2 units/mL) for 30–40 min at room temperature, and ruptured by sonication on ice (Crabb et al., 1998). Bacterial cells carrying the pET 3a vector and non-fusion rCRALBP were ruptured by sonication in 25 mM Tris pH 7, 10 mM sodium acetate containing protease inhibitors and reducing agent (0.1 mM PMSF, 0.5 mM leupeptin, 10 mM benzamidine, and 1 mM DTT-EDTA). Bacterial cells carrying the pET19b vector and fusion rCRALBP were lysed by sonication in 50 mM sodium phosphate buffer pH8, 300 mM sodium chloride (Ni-NTA buffer). The crude cell lysate was centrifuged (45,000 × *g* for 30 min at 4 °C) to remove debris and the protein concentration of the soluble cell lysate determined according to Lowry et al. (1951). The amount of rCRALBP in the soluble bacterial lysate was estimated from SDS-PAGE Coomassie Blue staining intensity and the protein concentration of the lysate.

Retinoid labeling and analysis

rCRALBP was labeled with retinoid in the bacterial cell lysate by adding a two- to threefold molar excess of 11-*cis*-Ral (or 9-*cis*-Ral) over rCRALBP [typically 1.2–1.8 μmol retinoid/1.2 L culture] and incubating in the dark at 4 °C for about 1 h. For labeling purified rCRALBP and purified bovine CRALBP, the proteins were dialyzed against 25 mM Tris Acetate, pH 7.5, 0.1 mM dithiothreitol and retinoids added to a twofold molar excess over CRALBP and incubated for 10 min at 4 °C. Retinoids were added from a concentrated solution (1–2 mg/mL) in ethanol (Carlson & Bok, 1992; Crabb et al., 1998). The identity and purity of retinoids used in labeling trials was verified by normal-phase HPLC using an 8 μ silica Dynamax-60A column (4.6 × 250 mm, Rainin Instrument Co.) and a Vista 5500 HPLC system (Varian, Palo Alto, CA). The retinoid binding functionality of rCRALBP was measured spectrophotometrically with a scanning spectrophotometer (Hitachi U-2000 spectrophotometer) or a J-600 circular dichroism spectropolarimeter (Jasco, Inc., Easton, MA). Retinoids were extracted from purified rCRALBP with 2 vol of hexane, the extract vacuum dried, resuspended in 100 μL ethanol, and analyzed by isocratic reverse-phase HPLC using a 5 μ Vydac C18 column (4.6 × 250 mm) equilibrated in 15 mM ammonium acetate pH 5 containing 66% acetonitrile and a flow rate of 2 mL/min. Retinoid labeling and holo CRALBP purification and characterization procedures were performed under dark-room conditions, with dim red

illumination to prevent photoisomerization of the retinoid to all-*trans*-retinaldehyde. Bleaching of rCRALBP samples was achieved by exposure to photography lights (150 W for ~10 min at ~40 cm distance at room temperature) or to ambient laboratory light for 30 min.

Purification of rCRALBP

Technical details for purifying rCRALBP have been described elsewhere (Crabb et al., 1998). Briefly, non-fusion rCRALBP was purified by three successive chromatography steps (DEAE cellulose, HTP and Mono Q HPLC) essentially as described by Saari and Bredberg (1988) for bovine retinal CRALBP. A Waters HPLC system (model 510 pumps and model 680 gradient controller) with a Beckman model 165 UV spectrophotometer were utilized for the Mono Q HPLC. Fusion rCRALBP was purified using nickel affinity chromatography on Ni-NTA agarose (Qiagen, Valencia, CA). Retinoid labeling of rCRALBP preparations was usually performed prior to purification as described above by adding either 11-*cis*-Ral or 9-*cis*-Ral to soluble lysate. For purifying fusion rCRALBP, an initial DEAE chromatography step was optionally used to remove excess retinoid before Ni-NTA chromatography. For all chromatographies, fractions were collected, absorbance measured at 280 nm and 425 nm for 11-*cis*-Ral–labeled rCRALBP (or 400 nm for 9-*cis*-Ral labeled rCRALBP), and fractions containing holo rCRALBP pooled based on purity by SDS-PAGE and absorbance spectra.

Molar extinction coefficients

Molar extinction coefficients were determined by recording the absorption spectrum for at least five different concentrations of purified holo rCRALBP in either water or 1 mM MOPS pH 7. Protein concentrations were determined by amino acid analysis and the average extinction coefficient values calculated using linear regression through zero protein concentration (Microsoft Excel 5.0 algorithm). Molar extinction coefficients determined for non-fusion holo rCRALBP with bound 11-*cis*-Ral were $\epsilon^{280nm} = 43{,}400$ M^{-1} cm^{-1} and $\epsilon^{425nm} = 13{,}400$ M^{-1} cm^{-1}. For holo rCRALBP with bound 9-*cis*-Ral, the determined extinction coefficients were $\epsilon^{280nm} = 44{,}600$ M^{-1} cm^{-1} and $\epsilon^{400nm} = 20{,}700$ M^{-1} cm^{-1}. Similar values have been reported for bovine CRALBP with bound 11-*cis*-Ral ($\epsilon^{280nm} = 42{,}000$ M^{-1} cm^{-1} and $\epsilon^{425nm} = 15{,}400$ M^{-1} cm^{-1}; Stubbs et al., 1979).

Electrophoretic and Western analyses

Sodium dodecyl sulphate-polyacrylamide gel electrophoresis (SDS-PAGE) was performed on 12% acrylamide gels according to Laemmli (1970) using a Mini-Protein II slab gel system (Bio Rad, Hercules, CA). Western analysis was performed using polyclonal anti-peptide antibodies specific for either the N-terminal 17 residues (S17L) or C-terminal 31 residues (S31F) of CRALBP as described elsewhere (Crabb et al., 1991).

Edman degradation, amino acid analysis, and mass spectrometry

Phenylthiocarbamyl amino acid analysis was performed using an automated analysis system (Applied Biosystems model 420H/130/920) (Crabb et al., 1997b). Protein sequence analysis by Edman degradation was performed using an Applied Biosystems gas phase sequencer (model 470/120/900) as previously described (Crabb et al., 1988a). Electrospray Mass Spectrometry and liquid chromatography ESMS (LC ESMS) were performed with a Perkin-Elmer Sciex API 300 triple quadrupole mass spectrometer (Concord, Ontario, Canada) fitted with an articulated ion spray plenum and an atmospheric pressure ionization source (Kapron et al., 1997). Initial tuning and calibration was with a standard mixture of polypropylene glycol from PE Sciex. Resolution was adjusted to about 50% valley between adjacent isotope peaks in a singly charged cluster, allowing singly charged ions to be identified by apparent spacing between peaks and doubly charged ions to be distinguished from those with higher charge states. Nitrogen was used as the nebulization gas (at 40 psi) and curtain gas and was supplied from a dewar (XL-45, Taylor Wharton) of liquid nitrogen (Merriam-Graves, Claremont, NH). LC ESMS were acquired in a positive ion mode at an orifice potential of 60 V over the scan range *m/z* 250–2,200 using 0.25 amu steps and a total scan time of 6 s. Synthetic peptides of known mass were used to verify correct calibration during LC ESMS. The HPLC eluant was split with 20% going to the mass spectrometer and the remainder collected in one-minute fractions. RP-HPLC for LC-ESMS was performed at a flow rate of 50 μL/min on a 5 μ Vydac C18 microbore column (1 × 250 mm) using an Applied Biosystems Model 120A HPLC system equipped with a 75 μL dynamic mixer and aqueous acetonitrile/trifluoroacetic acid solvents. Both intact rCRALBP and rCRALBP peptides were analyzed by LC ESMS. To verify the recombinant protein sequence, purified rCRALBP (39 μg) was reduced with dithiothreitol and alkylated with iodoacetamide in the presence of 8 M urea, 400 mM ammonium bicarbonate, pH 8. The carboxyamidomethylated protein (26 μg) was digested with trypsin in 1 M urea, 50 mM ammonium bicarbonate (3% trypsin by weight, overnight at 37 °C), and the tryptic digest analyzed by LC ESMS.

Circular dichroism

CD spectra in the far-UV (190–250 nm) and in the near-UV-visible (250–500 nm) ranges were recorded from a J-600 circular dichroism spectropolarimeter (Jasco Inc; Easton, Maryland). Spectra were recorded at 25 °C unless stated otherwise, with a scan speed of 100 nm/min, a time constant of 0.5 s, and a spectral band width of 1.0 nm. Quartz cells with path lengths of 1 cm or 0.25 mm were used for the near-UV-visible and far-UV CD measurements, respectively. Each spectrum was the average of 4 (near-UV-visible) or 16 (far-UV) scans. Thermal studies were performed in a cylindrical constant temperature quartz cell with a path length of 0.2 mm (Hellma; Jamaica, New York). Measurements were taken between 25 and 60 °C in 5 °C increments, with a 5-min equilibration time. The temperature inside the cell was calibrated with a bead thermometer and an accuracy of ±1 °C. Spectra were the average of eight scans. Mean residue ellipticity calculations were based on 316 amino acids per molecule of CRALBP. The composition of the secondary structural elements was calculated with LINCOMB algorithm (Perczel et al., 1992) software (Jasco).

Solution state NMR

^{19}F NMR spectra were obtained at 564 MHz on a Varian Unity 600 spectrometer equipped with a 5 mm $^{1}H/^{19}F$ probe. Biosynthetic incorporation of 5-fluorotryptophan (Sigma) into fusion rCRALBP

was achieved using defined bacterial growth medium as described elsewhere (Luck et al., 1997). 3-Fluorophenylalanine (−38.0 ppm) was used to calibrate the chemical shifts of fluorine resonances relative to trifluoroacetic acid at 0 ppm (Luck et al., 1997). All samples were adjusted to 10% D_2O (v/v) prior to analysis and spectra were acquired at 25 °C.

Supplementary material in the electronic appendix

The Electronic Appendix contains two folders entitled Supplementary Figures and Supplementary Mass Spectra. The Supplementary Figures folder contains four files: Supplementary Figure 1 (SDS-PAGE and Western Analysis of Non Fusion rCRALBP Expression), Supplementary Figure 2 (SDS-PAGE and Western Analysis of Fusion rCRALBP Expression), Supplementary Figure 3 (Purification of Non-Fusion rCRALBP) and Supplementary Figure 4 (Purification of Fusion rCRALBP). The Supplementary Mass Spectra folder contains 38 files (mass spectra) supporting Table 2 and titled by retention time as listed in Figure 1 and Table 2. Each supplementary mass spectra is labeled with the relevant rCRALBP peptide residue numbers.

Acknowledgments

Preliminary reports of this work were presented at the Sixth Symposium of the Protein Society, San Diego, California, July 1992: Crabb JW, Chen Y, Goldflam S, Johnson C, Intres R, West K. Recombinant cellular retinaldehyde binding protein, abstract M198; at The 65th Annual Meeting of the Association for Research in Vision and Ophthalmology, Sarasota, Florida, May 1993: Carlson A, Bok D, Crabb JW, Horwitz J. Circular dichroism analysis of native and recombinant cellular retinaldehyde-binding protein. Invest Ophthalmol *Vis Sci 34*:831, abstract 638; and at The Tenth Symposium of the Protein Society, August, 1996, San Jose, California, Luck L, Venters RA, Barrows S, Kapron JT, Crabb JW. 1996. ^{13}C and ^{19}F analysis of the CRALBP retinoid-binding pocket. *Protein Sci 5*:125, Suppl 1, abstract 396M. This study was supported in part by NIH grants EY06603, F32EY06271, EY444, EY331, EY3897, and EY7026, The Foundation Fighting Blindness, and NSF Grants DMB 8516111 and BIR 9115824. D.B. is Dolly Green Professor of Ophthalmology at UCLA and a Research to Prevent Blindness Senior Scientific Investigator. We thank Dr. Steven Carr, SmithKline Beecham Pharmaceuticals, for early assistance with mass spectrometry. NMR spectra were obtained with the help of Dr. Ronald Venters at Duke University, which is gratefully acknowledged. Instrumentation used in the Duke NMR Center was partially funded with grants from the NIH, NSF, and the North Carolina Biotechnology Center. We gratefully acknowledge valuable discussions with Dr. John Saari throughout the course of this work, and the assistance of Charles Johnson with protein purification, Drs. Kyusung Park and Lukasz Salwinski with the LINCOMB algorithm, and Valerie Oliver and Marina LaDuke in manuscript preparation.

References

Adler AJ, Evans CD, Stafford WF III. 1985. Molecular properties of bovine interphotoreceptor retinol-binding protein. *J Biol Chem 260*:4850–4855.

Asenjo AB, Rim J, Oprian DD. 1994. Molecular determinants in human red/green color discrimination. *Neuron 12*:1131–1138.

Brown PK, Wald G. 1956. The neo-b isomer of vitamin A and retinene. *J Biol Chem 222*:865–877.

Carlson A, Bok D. 1992. Promotion of the release of 11-*cis*-retinal from cultured retinal pigment epithelium by interphototreceptor retinoid-binding protein. *Biochemistry 31*:9056–9062.

Chen Y, Johnson C, West K, Goldflam S, Bean MF, Huddleston MJ, Carr SA, Gabriel JL, Crabb JW. 1994. Mapping the retinoid-binding domain of cellular retinaldehyde-binding protein. In: Crabb JW, ed. *Techniques in protein chemistry V*. San Diego: Academic Press. pp 371–378.

Cowan SW, Newcomer ME, Jones TA. 1993. Crystallographic studies on a family of cellular lipophilic transport proteins. Refinement of P2 myelin protein and the structure determination and refinement of cellular retinol-binding protein in complex with all-*trans*-retinol. *J Mol Biol 230*:1225–1246.

Cowan SW, Newcomer ME, Jones TA. 1990. Crystallographic refinement of human serum retinol binding protein at 2Å resolution. *Proteins 8*:44–61.

Crabb JW, Johnson CM, Carr SA, Armes LG, Saari JC. 1988a. The complete primary structure of the cellular retinaldehyde-binding protein from bovine retina. *J Biol Chem 263*:18678–18687.

Crabb JW, Goldflam S, Harris SE, Saari JC. 1988b. Cloning of the cDNAs encoding the cellular retinaldehyde-binding protein from bovine and human retina and comparison of the protein structures. *J Biol Chem 263*:18688–18692.

Crabb JW, Gaur VP, Garwin GG, Marx SV, Chapline C, Johnson CM, Saari JC. 1991. Topological and epitope mapping of the cellular retinaldehyde-binding protein from retina. *J Biol Chem 266*:16674–16683.

Crabb JW, Chen Y, Kapron JT, West KA, Bredberg DL, Saari JC. 1996. Analysis of the retinoid-binding site of CRALBP. *Invest Ophthal Vis Sci 37*:3691, S802.

Crabb JW, Roth KE, Pradis S, Luck LA, Venters RA, Spicer LD. 1997a. Mutational mapping of the retinoid binding-pocket in the cellular retinaldehyde-binding protein (CRALBP). *Protein Sci 6(Suppl 2)*:67,76.

Crabb JW, Chen Y, Goldflam S, West K, Kapron J. 1998. Methods for producing recombinant human cellular retinaldehyde-binding protein. In: Redfern C, ed. *Methods in molecular biology, vol 89, retinoid protocols*. Totowa, New Jersey: Humana Press. pp 91–104.

Crabb JW, West KA, Dodson WS, Hulmes JD. 1997c. Amino acid analysis. In: Coligan JE, Ploegh HL, Smith JA, Speicher DW, eds. *Current protocols in protein science*, Unit 11.9 (Supplement 7). New York: John Wiley & Sons, Inc. pp 11.9.1–11.9.42.

Futterman S, Saari JC, Blair S. 1977. Occurrence of a binding protein for 11-*cis*-retinal in retina. *J Biol Chem 252*:3267–3271.

Gu M, Warshawsky I, Majerus PW. 1992. Cloning and expression of a cytosolic megakaryocyte protein–tyrosine–phosphatase with sequence homology to retinaldehyde-binding protein and yeast SE14p. *Proc Natl Acad Sci USA 89*:2980–2984.

Hubbard R. 1956. Geometrical isomerization of vitamin A, retinene and retinene oxime. *J Am Chem Soc 78*:4662–4667.

Intres R, Goldflam S, Cook JR, Crabb JW. 1994. Molecular cloning and structural analysis of the human gene encoding cellular retinaldehyde-binding protein from retina. *J Biol Chem 266*:16674–16683.

Kapron JT, Hilliard G, Lakins J, Tenniswood M, West KA, Carr SA, Crabb JW. 1997. Identification and characterization of glycosylation sites in human serum clusterin. *Protein Sci 6*:2120–2133.

Laemmli UK. 1970. Cleavage of structural proteins during the assembly of the head of bacteriophage T4. *Nature 227*:680–685.

Lowry OH, Rosebrough NJ, Farr AL, Randall RJ. 1951. Protein measurement with the Folin phenol reagent. *J Biol Chem 193*:265–275.

Luck LA, Barrows SA, Venters RA, Kapron J, Roth KA, Paradis SA, Crabb JW. 1997. NMR methods for analysis of CRALBP retinoid-binding. In: Marshak D, ed. *Techniques in protein chemistry VIII*. San Diego: Academic Press. pp 439–448.

Oroshnik W. 1956. The synthesis and configuration of neo-b vitamin A and neoretinene b. *J Am Chem Soc 78*:2651–2652.

Maw MA, Kennedy B, Knight A, Bridges R, Roth KE, Mani EJ, Mukkadan JK, Nancarrow D, Crabb JW, Denton MJ. 1997. Mutation of the gene encoding cellular retinaldehyde binding protein in autosomal recessive retinitis pigmentosa. *Nat Genet 17*:198–200.

Ozaki K, Terakita A, Ozaki M, Hara R, Hara T, Hara-Nishimura I, Mori H, Nishimura M. 1994. Molecular characterization and functional expression of squid retinal-binding protein, a novel species of hydrophobic ligand-binding protein. *J Biol Biochem 269*:2828–2845.

Perczel A, Park K, Fasman GD. 1992. Analysis of the circular dichroism spectrum of proteins using the convex constraint algorithm: A practical guide. *Anal Biochem 203*:83–93.

Saari JC, Bredberg DL. 1982. Enzymatic reduction of 11-*cis*-retinal bound to cellular retinal-binding protein. *Biochim Biophys Acta 716*:266–272.

Saari JC, Bredberg DL, Garwin GG. 1982. Identification of the endogenous retinoids associated with three cellular retinoid-binding proteins from bovine retina and retinal pigment epithelium. *J Biol Chem 257*:13329–1333.

Saari JC, Bredberg DL. 1987. Photochemistry and stereoselectivity of cellular retinaldehyde-binding protein from bovine retina. *J Biol Chem 262*:7618–7622.

Saari JC, Bredberg DL. 1988. Purification of cellular retinaldehyde binding protein from bovine retina and retinal pigment epithelium. *Exp Eye Res 46*:569–578.

Saari JC, Bredberg DL, Noy N. 1994. Control of substrate flow at a branch in the visual cycle. *Biochemistry 33*:3106–3112.

Saari JL, Huang J, Possin DE, Fariss RN, Leonard J, Garwin GG, Crabb JW,

Milam AH. 1997. Cellular retinaldehyde-binding protein is expressed by oligodendrocytes in the optic nerve and brain. *Glia 21*:259–268.

Salama SR, Cleves AE, Malehorn DE, Whitters EA, Bankaitis VA. 1990. Cloning and characterization of Kluyveromyces lactis SEC14, a gene whose product stimulates Golgi secretory function in *Saccharomyces cervisiae*. *J Bacteriol 172*:4510–4521.

Sandhu GS, Precup JW, Kline BC. 1989. Rapid one-step characterization of recombinant vectors by direct analysis of transformed *Escherichia coli* colonies. *Biotechniques* 7:689–670.

Sato Y, Arai H, Miyata A, Tokita S, Yamamoto K, Tanabe T, Inoue K. 1993. Primary structure of α-tocopherol transfer protein from rat liver. *J Biol Chem 268*:17705–17710.

Stubbs GW, Saari JC, Futerman S. 1979. 11-*cis*-retinal-binding protein from retina, isolation and partial characterization. *J Biol Chem 254*:8529–8533.

Studier FW, Rosenberg AH, Dunn JJ, Dubendorff JW. 1990. Use of T7 RNA polymerase to direct expression of cloned genes. *Methods Enzymol 185*:60–89.

Wagner G, Wuthrick K. 1986. Observation of internal motility by nuclear magnetic resonance in solution. *Methods Enzymol 131*:307–326.